Published in final edited form as:
Nanotoxicology. 2014 August ; 8(5): 533–548. doi:10.3109/17435390.2013.803624.

Three human cell types respond to multi-walled carbon nanotubes and titanium dioxide nanobelts with cell-specific transcriptomic and proteomic expression patterns

Susan C. Tilton[*], **Norman J. Karin**[*], **Ana Tolic**[*], **Yumei Xie**[*], **Xianyin Lai**[†], **Raymond F. Hamilton Jr.**[‡], **Katrina M. Waters**[*], **Andrij Holian**[‡], **Frank A. Witzmann**[†], and **Galya Orr**[*,1]

[*]Environmental Molecular Sciences Laboratory, and Fundamental & Computational Sciences Directorate, Pacific Northwest National Laboratory, Richland, Washington 99352

[†]Department of Cellular and Integrative Physiology, Indiana University School of Medicine, Indianapolis, Indiana 46202

[‡] Center for Environmental Health Sciences, Department of Biomedical and Pharmaceutical Sciences, University of Montana, Missoula, Montana 59812

Abstract

The growing use of engineered nanoparticles (NPs) in commercial and medical applications raises the urgent need for tools that can predict NP toxicity. We conducted global transcriptome and proteome analyses of three human cell types, exposed to two high aspect ratio NP types, to identify patterns of expression that might indicate high vs. low NP toxicity. Three cell types representing the most common routes of human exposure to NPs, including macrophage like (THP-1), small airway epithelial (SAE), and intestinal (Caco-2/HT29-MTX) cells, were exposed to TiO_2 nanobelts (TiO_2-NB; high toxicity) and multi-walled carbon nanotubes (MWCNT; low toxicity) at low (10 μg/ml) and high (100 μg/ml) concentrations for 1 and 24 h. Unique patterns of gene and protein expressions were identified for each cell type, with no differentially expressed ($p<0.05$, 1.5-fold change) genes or proteins overlapping across all three cell types. While unique to each cell-type, the early response was primarily independent of NP type, showing similar expression patterns in response to both TiO_2-NB and MWCNT. The early response might therefore indicate a general response to insult. In contrast, the 24 h response was unique to each NP type. The most significantly ($p<0.05$) enriched biological processes in THP-1 cells indicated TiO_2-NB regulation of pathways associated with inflammation, apoptosis, cell cycle arrest, DNA replication stress and genomic instability, while MWCNT regulated pathways indicating increased cell proliferation, DNA repair and anti-apoptosis. These two distinct sets of biological pathways might therefore underlie cellular responses to high and low NP toxicity, respectively.

Keywords

biological pathway; biological network; differential gene regulation; differential protein regulation; high aspect ratio nanomaterial

[1] Corresponding Author: Galya Orr, galya.orr@pnnl.gov Environmental Molecular Sciences Laboratory Pacific Northwest National Laboratory P.O. Box 999 MS: K8-88 Richland, WA 99352 Tel: 509 371-6127 Fax: 509 371-6145.

Introduction

High aspect ratio nanoparticles (NPs) such as nanotubes, nanowires and nanobelts are utilized with growing frequency for a wide variety of industrial applications because of the unique physical and chemical properties afforded by these shapes. For example, multi-walled carbon nanotubes (MWCNT) have novel properties that make these structures highly attractive for use in superconductor materials, optical devices and biomedical applications. . Metal oxide nanobelts are employed in the manufacture of devices such as field-effect transistors, gas sensors, nanoresonators, and nanocantilevers, and TiO_2 nanobelts (TiO_2-NB) are being explored as photocatalysts (Wang *et al.* 2009). With this increase in commercial use comes the concomitant elevation in likelihood of occupational and consumer exposures, and the growing concern about the potential risks posed by high aspect ratio NPs to human and environmental health (Donaldson *et al.* 2011; Helland *et al.* 2007; Pacurari *et al.* 2010).

Because of their structural similarity to asbestos fibers, a rather extensive literature exists with respect to the toxicity of carbon-based high aspect ratio NPs (Helland *et al.* 2007; Pacurari *et al.* 2010; Shvedova *et al.* 2009). Nonetheless, there is no clear consensus as to their safety or the mechanisms underlying the response that they elicit. For example, MWCNT had cytotoxic effects equivalent to chrysotile asbestos when tested in human A549 lung epithelial cells and macrophages (human THP-1 and mouse RAW 264.7) in vitro (Soto *et al.* 2007). In contrast, acute (3 days) treatment of A549 lung epithelial cells with MWCNT led to reactive oxygen species production and decreases in mitochondrial function (MTT assay), but no genotoxicity or alterations in cell proliferation (Thurnherr *et al.* 2011). Long-term (6 months) exposure of these cells to MWCNT had no apparent effects on cell viability despite significant uptake of nanotubes. Chronic exposure to MWCNT also did not predispose the cells to cytotoxic effects of subsequent acute treatments to MWCNT or other nanoparticles (Thurnherr *et al.* 2011). Similarly, Pulskamp et al. found that MWCNT did not elicit acute toxicity in cultured macrophage and lung epithelial cell lines (Pulskamp *et al.* 2007). Both single-walled carbon nanotubes (SWCNT) and MWCNT elicited equivalent cytotoxic effects in RAW 264.7 macrophages (Murr *et al.* 2005). In contrast, although MWCNT reduced the viability of guinea pig alveolar macrophages, their response was less severe than the response induced by SWCNT (Jia *et al.* 2005). Similarly, exposure of renal epithelial cells to SWCNT in vitro led to robust decreases in transepithelial electrical resistance, a sensitive measure of cell viability, while MWCNT treatments were less impactful (Blazer-Yost *et al.* 2011). Efforts to characterize the respiratory toxicity of MWCNT in laboratory animals in vivo also have led to contradictory results (reviewed in Shvedova *et al.* 2009).

TiO_2 NPs historically have been considered to be relatively harmless and are widely used as a component of sunscreens and toothpastes and as a cosmetic pigment (reviewed in Iavicoli *et al.* 2011). However, as discussed above for high aspect ratio carbon NPs, the shape and aspect ratio of NPs can render biologically inert substances cytotoxic, particularly in the context of inhalation (Donaldson *et al.* 2011). TiO_2 nanowires and multiwalled TiO_2 nanotubes elicited cytotoxic effects in H596 human lung tumor cell line (Magrez *et al.* 2009), and fibrous, but not particulate, TiO_2 caused cytotoxicity in rat alveolar macrophages

in vitro (Watanabe *et al.* 2002). Long (> 15 μm), but not short (< 5 μm) anatase TiO_2-NB caused an inflammatory response and cytotoxicity in mouse alveolar macrophages, likely by a process linked to lysosomal damage and NLRP3 inflammasome activation (Hamilton *et al.* 2009). In contrast, the transient inflammatory response of rats to pulmonary instillation of nanorods composed of anatase TiO_2 did not differ from that measured in animals treated with TiO_2 in either nanodot (~6 nm) or fine (300 nm) forms (Warheit *et al.* 2006).

While some of these reported differences in toxicity may be due to the fact that NP properties are strongly modulated by the environment and can change with different exposure conditions, protocols or material source (Karakoti *et al.* 2012; Oberdörster *et al.* 2005), it is also likely that NP exposures elicit cell type-specific responses determined by the cellular physiology and the distinct extra- and intra-cellular environments. Guided by the working hypothesis that the same NPs can elicit diverse cell-specific responses, and that distinct pathways are activated in response to NPs with distinct levels of toxicity, we studied the cellular response of three different human cell-types, likely to be impacted by NP exposure, to two high aspect ratio NPs, known to induce low or high level of toxicity. The studies were conducted under identical exposure conditions and using the exact same NPs, reagents and protocols to ensure that the cells are exposed to the same NP properties and that any detected differences in cellular response are physiologically relevant. We utilized unbiased analyses of global gene and protein expression, which offer sensitive tools for identifying the broad range of potential responses. This approach allowed us to decipher differences in cellular responses to the exact same particle properties and identify mechanisms underlying high vs. low NP toxicity of high aspect ratio NPs.

Materials and Methods

Experimental design

The most common routes of significant human exposure to NPs are inhalation and ingestion. Among the first cells to encounter inhaled NPs are the lung epithelia, and cells that line the gastrointestinal tract are predominant targets of ingested NPs. Immune surveillance cells in the monocyte/macrophage lineage are also involved in the responses to inhaled and ingested NPs. Therefore, three human cell lines were chosen in this study to represent the cells most likely to be impacted by NP exposure, including macrophage-like THP-1 cells, primary small airway epithelial (SAE) cells and Caco-2/HT29-MTX co-cultures. Caco-2 cell line was recommended by the International Life Science Institute Nanomaterial Toxicity Screening Working Group as a model of human intestinal epithelia (Wikmanlarhed and Artursson 1995). The inclusion of the goblet cell line, HT29-MTX, in co-culture further increases the similarity of this in vitro system to intestinal function in vivo (Walter *et al.* 1996; Wikmanlarhed and Artursson 1995). Their combination provides a physiologically relevant system characterized by tight junctions and considerable mucus secretion (Mahler *et al.* 2009). SAE cells are commercially available human primary cells that can be cultured for a limited number of passages. These cells represent more closely the epithelial cells lining the respiratory tract when compared with transformed cell lines. The cells are isolated 1 mm beyond the bronchial tubes in small airways, which largely include the alveolar region. This region consists mainly of alveolar type I epithelial cells and to a lesser extent of

type II epithelial cells. Airborne NPs that enter the respiratory tract are likely to be deposited in this region Donaldson *et al*. 2008; Mercer *et al*. 2010), where alveolar epithelial cells present a vulnerable target cell type. THP-1 cells are of human origin and are often used as a macrophage model in toxicology studies (Hamilton et al. 2012; Verma et al. 2012; Xia *et al.* 2013) instead of primary human alveolar macrophages that can only be obtained by lung lavage from volunteers. The study focused on two high aspect ratio NPs, MWCNTs and TiO_2-NBs, which were investigated by the NIEHS consortium in an effort to establish screening assays (Xia *et al.* 2013). Observations by the consortium showed lower and higher toxicity levels for MWCNTs and TiO_2-NBs, respectively, when tested in alveolar type II (RLE-6TN) and bronchial (BEAS-2B) epithelial cell lines, and in the THP-1 cell line (Xia *et al.* 2013). These NPs were chosen to enable the comparison of responses to fibrous NPs with distinct levels of toxicity. Because of the magnitude of this study, NP doses for cell exposure were limited to two, low and high, NP concentrations. The study was also limited to two, early (1 h or 3h) and late (24 h), time points post exposure, to identify initial and more developed responses, respectively. Because transcriptional regulatory events typically precede protein changes, we chose to stagger the measurement of genes and proteins at the early time point, 1 h and 3 h, respectively. The experimental design is summarized in Table I. Detailed descriptions of the growth conditions, exposure and harvesting protocols for each cell type are provided in the Supplementary Methods File.

Nanoparticle Dispersion—Purified MWCNT were weighed and added to an autoclavable glass tube with a screw cap; water was added to make a 5 mg/ml suspension. The MWCNT were vortexed for 5 s and sonicated for 15 min in a water bath sonicator. Immediately after sonication, an aliquot (160 μl) was removed for dilution in culture medium (3.84 ml) to prepare a 200 μg/ml stock solution, from which 100 μg/ml and 10 μg/ml media mixtures were prepared for the exposures. TiO_2-NB were weighed and added to an autoclavable glass tube with screw cap and magnetic stir bar; 7.5% BSA in DPBS was added to make a 5 mg/ml suspension. TiO_2-NB were stirred by magnetic stir plate for 1 h. Each sample was gently vortexed to make further dilutions in medium as described above for MWCNT.

Nanoparticle characterization

TiO_2-NB—The TiO_2-NB were synthesized as described earlier in (Hamilton *et al.* 2009). Their length was 7 μm, width was 0.2 μm and thickness was 0.01 μm, as measured from transmission electron microscopy (TEM) images, such as the image shown in Figure 1. XRD analysis confirmed that the TiO_2-NB consisted of 100% anatase, and BET measurements showed surface area of 17.94 m^2g^{-1}. Table II summarizes the size and zeta potential values measured by Dynamic Light Scattering (DLS) and Zetasizer, respectively, in water, RPMI and DMEM growth media supplemented with 10% FBS, as well as in supplemented SABM medium. The three growth media were used for THP-1, Caco-2/HT29-MTX and SAE cells, respectively (Supplementary Methods File). It is important to note that DLS provides a rough size distribution for non-spherical particles.

MWCNT—MWCNT (OD 20-30nm, Purity 95%) were purchased from Cheap Tubes Inc. (Brattleboro VT). Residual metal catalysts and carbonaceous impurities were removed using

a microwave-induced controlled method (Chen and Mitra 2008). MWCNT thus retain their chemical and physical properties and are not functionalized. Detailed characterization of these MWCNT can be found in Wang et al., 2010 (Wang *et al.* 2010). Primary size measured by TEM showed length of 5-10 nm and diameter of 20-30 nm. Surface area measured by BET was 513 m^2g^{-1}, and elemental analysis showed 1.8% Ni and 0.1% Fe. Size measured by DLS and zeta potential measured by Zetasizer in water and in the three growth media listed above are summarized in Table II.

Toxicity assessment

Cell Viability—CellTiter 96® AQ_{ueous} non-radioactive cell proliferation assay (Promega, Madison, WI) was used to quantify cell viability 1 h and 24 h post exposure. A detailed protocol can be found in Xie *et al.* 2012. The mean absorbance of negative control, where cells were exposed to solution containing no NPs, was established as 100% cellular viability. The absorbance of cells exposed to the NPs (minimum of 3 biological replicates per condition) was measured and normalized to negative control. Significant change in the normalized values was determined using a one-way ANOVA comparing exposed cells to negative control with Dunnett's test and presented as the mean ± standard error of the mean (*SEM*), with significance indicated at $P < 0.05$ (*), 0.01 (**) or 0.001 (***).

Membrane Integrity—Cyto Tox 96® non-radioactive cytotoxicity assay (Promega, Madison, WI) was used to quantify LDH release at 6 and 24 h post exposure. A detailed protocol can be found in Xie *et al.* 2012. Absorption values in cells exposed to the NPs (minimum of 3 biological replicates per condition) were measured and normalized to lysed 100% kill cells and significance was determined relative to the time-matched negative control, cells exposed to no particles, using one-way ANOVA with Dunnett's test and presented as the mean ± standard error of the mean (*SEM*), with significance indicated at $P < 0.05$ (*), 0.01 (**) or 0.001 (***).

Transcriptomics analysis

Global transcriptomics were conducted for each cell type 1 and 24 h post exposure to 10 or 100 μg/ml MWCNT or TiO_2-NB (n=3 biological replicates per condition). The time points for data collection were chosen based on the cytotoxicity measurements (Figure 2) showing little to no toxicity early after exposure (1 h) and NP-specific toxicity (20-40%) at later time points (24 h). Detailed protocols are available in the Supplementary Methods File. Briefly, total RNA was isolated and biotin-labeled cRNA was synthesized and fragmented using Affymetrix 3' IVT Express reagents for hybridization to Human Genome U133A 2.0 GeneChips (Affymetrix, Santa Clara, CA).

Raw intensity data were quantile normalized by Robust Multi-Array Analysis (RMA) summarization (Bolstad *et al.* 2003) and transformed to cell- and time-specific controls. Data were analyzed by ANOVA unequal variance with Tukey's multiple corrections test and 5% false discovery rate calculation (Benjamini and Hochberg 1995) using GeneSpring v.11 (Silicon Genetics, Redwood City, CA). Significant genes were filtered to include those that met the criteria of $p<0.05$ and ≥1.5-fold expression for each treatment group compared to

time- and cell-matched controls. Raw and normalized Affymetrix data files are available online through the GEO database (GSE42069).

Quantitative RT-PCR analysis

Real time quantitative reverse transcriptase polymerase chain reaction (qRT-PCR) was used to verify selected gene expression changes revealed by Affymetrix microarray analysis (details in Supplementary Methods File). To further ensure the specificity of the amplifications, primer pairs (Supplementary Table S1) were designed to span introns except for the genes that had intron-exon structures that did not allow this. Relative expression was determined using the $\Delta\Delta C_T$ method with samples normalized to the expression level of the cyclophilin A transcript, the product of the human PPIA gene. All analyses were performed on n=3 samples.

Proteomics analysis

Global proteomics were conducted for each cell type 3 and 24 h post exposure to 10 or 100 μg/ml MWCNT or TiO_2-NB (n=5 biological replicates per condition). The reasons for selecting these parameters are described earlier under Experimental design and Transcriptomics analysis. Details of the sample preparation, global protein identification and quantitation are available in the Supplemental Methods Files. Briefly, cell lysates were tryptic digested for global LCMS/MS analysis. Proteins were identified against the International Protein Index (IPI) database (ipi.HUMAN.v3.69) using SEQUEST (v. 28 rev. 12) and validated by PeptideProphet (Keller *et al.* 2002) and ProteinProphet (Nesvizhskii *et al.* 2003) in the Trans-Proteomic Pipeline (TPP, v. 3.3.0). Only proteins and peptides with (a) protein probability ≥ 0.9000, (b) peptide probability ≥ 0.8000, and (c) peptide weight ≥ 0.5000 were used in the quantitation algorithm and are represented in Supplementary Figure S1 as “All identified peptides.” Protein abundance was determined using a label-free platform, IdentiQuantXL™ (Lai *et al.* 2011). Significance was calculated by Student's T-test with 5% false discovery rate estimation (Storey 2002). Significant proteins were filtered to include those that met the criteria of $p<0.05$ and ≥1.5-fold abundance for each treatment group compared to time- and cell-matched controls.

Bioinformatics

Unsupervised hierarchical clustering of microarray data was performed using Euclidean distance metric and centroid linkage clustering to group gene expression patterns by similarity. The clustering algorithms, heat map visualizations and centroid calculations were performed with Multi-Experiment Viewer (Saeed *et al.* 2003) software based on log2 expression ratio values. Venn diagrams were created from the comparison of significant genes or proteins across treatment group, cell type or time point. Comparison across transcriptomic gene lists was performed using GeneSpring (Silicon Genetics) and across proteomic abundance lists using Bioinformatics Resource Manager v2.2 (Tilton *et al.* 2012). Functional enrichment statistics and pathway analysis were determined with Metacore (GeneGo, Thomson Reuters, New York, NY) to identify the most significant ($p<0.05$) processes affected by nanoparticle treatment. The statistical scores in MetaCore are calculated using a hypergeometric distribution where the *p* value essentially represents the

probability of a particular mapping arising by chance, given the number of genes or proteins in a biological process from the experimental dataset compared to all the genes or proteins in that process available for the background dataset. For the transcriptional data, the background dataset included all of the genes on the Affymetrix Human Genome U133 Plus 2.0 chip. For the proteomic data, the background dataset included all of the proteins detected in the cells by global LC-MS/MS.

Results

Toxicity Assessment

Cytotoxicity of two high aspect ratio NPs, MWCNT and TiO_2-NB was measured in three human cell types, chosen to represent the cells most likely to be impacted by NP exposure via inhalation (SAE cells) or digestion (Caco-2/HT29-MTX cell), as well as immune surveillance cells (THP-1 cells). To confirm the response pattern observed previously in THP-1 cells (Xia et al. 2013) and determine the response in SAE and Caco-2/HT29-MTX cells, MTS conversion to formazan and LDH release were quantified to assess cell viability and membrane integrity, respectively. The results are presented in Figures 2 and summarized in Supplementary Table S2, where significance, indicated at $P < 0.05$ (*), $P < 0.01$ (**) or $P < 0.001$ (***), was determined using a one-way ANOVA and presented as the standard error of the mean (SEM).

For MWCNT, no toxicity was observed at 1 h post exposure and a low level of toxicity (<20% change, $p<0.05$) was observed at 24 h post exposure only in response to the high concentration of 100 μg/ml in all three cell types. In contrast, TiO_2-NB elicited higher levels of toxicity (20-40% change, $p<0.01$) at 24 h in both THP-1 and SAE cells. However, only low levels of toxicity were observed in the Caco-2/HT29-MTX cells.

Cells responded to NP exposure with unique cell-specific gene and protein expression patterns

Overall, 1479 genes and 537 proteins were differentially expressed ($p<0.05$, 1.5-fold change) in all treatment groups compared to time- and cell-matched controls (Supplementary Table S3). When sorted by NP- and cell-types, none of these genes or proteins were found to be differentially regulated in common across all three cell types in response to either MWCNT or TiO_2-NB, and only few were differentially regulated in common across any two cell types (Figure 3A and 3B). These observations indicated that the cells responded to the NPs with unique sets of genes and proteins, likely reflecting the distinct transcriptome/proteome and physiology of each cell type.

It should be noted that the number of genes and proteins differentially expressed under each treatment condition (Supplementary Table S3) did not correlate with toxicity observed in vitro (Figure 2). For example, the most cytotoxic exposure (100 μg/ml TiO_2-NB in SAE cells after 24 h) did not result in the greatest number of differentially regulated genes and proteins. These data suggest that the global omic measurements were associated with exposure-specific responses indicative of mechanism of action instead of overt toxicity

Unsupervised hierarchical clustering of all differentially regulated genes was utilized to define trends in gene expression across particle type, cell type, dose and time. Clustering of the data in Figure 4 showed the unique cell specific patterns of expression for each NP type, dose and exposure time. The response in THP-1 cells was concentration-, time- and particle type-dependent with most genes differentially regulated at the 100 μg/ml, 24 h treatment groups. There were fewer genes deregulated in SAE and Caco-2/HT29-MTX cells compared to THP-1 cells overall at the time-points measured. In SAE cells, most genes were differentially regulated at 1 h time-point with common patterns of expression observed in response to both MWCNT and TiO_2-NB. In Caco-2/HT29-MTX cells, common patterns of expression to both NP types were also observed at 1 h, with the majority of genes differentially regulated at 24 h in response to TiO_2-NB.

Quantitative RT-PCR was utilized to validate the microarray analysis for a subset of genes identified in the global transcriptomic dataset as being differentially regulated in either cell- or NP-specific manner. Transcripts differentially regulated in Caco-2/HT29-MTX and SAE cells in response to 1 h NP exposure (Supplementary Figure 2), transcripts differentially regulated in THP-1 cells in response to 24 h NP exposure (Supplementary Figure 3), and those showing NP-specific regulation (Supplementary Figure 4) were analyzed by qRT-PCR, showing responses similar to those observed by microarray analysis.

Cells responded to NP exposure by differentially regulating both common and unique sets of biological processes

We further determined whether the NPs impacted common biological processes in the three cell types. Also, since little direct overlap between genes and proteins from the transcriptomic and proteomic datasets was observed, and since we expect differential regulation of genes and proteins within the same pathway, we looked for overlap between the transcriptomic and proteomic datasets at the function/pathway level. Functional enrichment statistics and pathway analysis of the transcriptomics and proteomics data were used to identify significantly ($p<0.05$) regulated biological processes in response to each NP type, and compare these processes across cell types. Figures 5A shows significantly regulated functions that are common between genes and proteins across all treatments. Figure 5B shows biological processes that are uniquely enriched for either the proteomic or transcriptomic data. In these figures, the level of significance for each process (*P*-value) is shown in a heatmap on a scale from non-significant (black) to highly significant (blue; $p<0.001$) based on the level of enrichment of each process in the datasets.

Overall, we observed several important processes differentially regulated in common across the cell types and in common between transcriptomics and proteomics after NP exposure (Figure 5). For example, after exposure to TiO_2-NB, approximately 75% of all significantly regulated transcriptomic processes were common across any two cell types and ~10% of the processes were common across all three cell types. The four biological processes significantly enriched at the transcriptional level across all cell types after TiO_2-NB exposure include Apoptotic nucleus, G1-S growth factor regulation, Regulation of angiogenesis and Regulation of epithelial-tomesenchymal transition (Figures 5A and 5B), which might describe a common response mechanism to TiO_2-NB. Fewer common

differentially regulated biological processes were identified after MWCNT exposure. The only process significantly regulated in all cell types after MWCNT exposure was related to platelet-endothelium-leukocyte interactions during cell adhesion (Figure 5B). These data show that even though none of the same genes were differentially expressed across the cell types, there were some common pathways associated with TiO_2-NB or MWCNT exposure.

Functional analysis of the global proteomic data identified no differentially regulated biological processes in common across all three cell types after TiO_2-NB exposure and only one process, Inflammation_IL-6 signaling, in common afer MWCNT exposure. However, most of the processes significantly enriched in the proteomic dataset were also significantly enriched at the transcriptional level. Of interest was the Apoptotic nucleus process, which was significantly regulated at both the gene and protein levels only after TiO_2-NB exposure (Figure 5A). These observations suggest that the apoptotic nucleus process might be an important mechanism unique to TiO_2-NB exposure independent of cell type. Therefore, we investigated this process in more detail by creating an integrated network of the differentially expressed genes (red circles) and proteins (blue circles) using direct interactions between the nodes from the two datasets (Figure 5C). The signaling network, which is mediated by NF-κB and includes genes associated with apoptosis and DNA repair, may provide a mechanism for differential toxicity between the two NP types.

Another interesting differentially regulated biological process, the immune response - antigen presentation process (Figure 5B), was unique to the proteomic data and was shared by THP-1 and SAE cells after both TiO_2-NB and MWCNT exposures. This process might represent a general response to NPs in these two cell types. A closer look at the proteins listed under the antigen presentation process (Supplementary Figure S5) revealed proteins that were commonly regulated by both NP types in all three cell types, supporting the idea that this process is involved in the general response mechanism to NPs, or the recognition of a foreign object in these cells.

Early response was common across NP types, while late response was NP-specific - mostly in response to TiO_2-NB

Sorting all differentially expressed genes by time post exposure (Figure 6) revealed that each cell type responded with an early (1 h, left panel) transcriptional response that was common across NP types. In contrast, the late response (24 h, right panel) was unique to each NP type with most genes differentially regulated by TiO_2-NB. The Venn diagrams in Figure 6 reveal that only few differentially expressed genes were common between the early and late time points, indicating distinct response patterns over time. At 1 h post exposure, THP-1 (Figure 6A), SAE (Figure 6B) and Caco-2/HT29-MTX (Figure 6C) cells responded with 38, 289 and 80 differentially expressed ($p<0.05$, 1.5-fold change) genes, respectively, compared to time- and cell-matched controls. Both the direction and magnitude of gene expression was similar between TiO_2-NB and MWCNT exposures suggesting that the early transcriptional response is general to NP exposure. The most significantly regulated biological processes common to MWCNT and TiO_2-NB at the early (1 h) time point are listed in Supplementary Table S4. The common early response to MWCNT and TiO_2-NB was supported by the 3 h

proteomics data set (Figure 7), showing similar patterns of differentially expressed ($p<0.05$, 1.5-fold change) proteins in response to both NPs in each cell type.

In contrast, gene expression data at 24 h post exposure revealed that each cell type responded with distinct NP-specific gene expression patterns (Figure 6, right panel). THP-1 (Figure 6A), SAE (Figure 6B) and Caco-2/HT29-MTX (Figure 6C) cells responded with 1102, 56 and 244 differentially expressed genes, respectively, showing unique expression patterns in response to MWCNT or TiO_2-NB. Further, most of the genes at 24 h were differentially regulated by TiO_2-NBs, particularly in SAE and Caco-2/HT29-MTX cells, suggesting that the effect of MWCNT exposure in these cells was transient. Only THP-1 cells showed significantly regulated biological processes in response to both MWCNT and TiO_2-NB (Supplementary Table S4).

Late response in THP-1 cells was NP-specific and might describe mechanisms underlying high (TiO_2-NB) and low (MWCNT) levels of toxicity

THP-1 cells responded to MWCNT and TiO_2-NB at 24 h with distinct sets of differentially expressed genes and biological processes (Figure 8). Of the 812 genes significantly regulated ($p<0.05$, 1.5-fold change) by TiO_2-NB and the 406 genes significantly regulated by MWCNT, 134 were regulated in common by the two NP types (Figure 8A).

These genes were used to identify biological processes that were significantly regulated by MWCNT, TiO_2-NB or both NP types using MetaCore (GeneGo). The most significantly regulated biological processes comprised of the common genes included chemotaxis, immune response involved cytokines, and apoptosis functions (Figure 8B, common). The most significantly regulated biological processes in response to MWCNT showed regulation of processes important for DNA damage - checkpoint and repair, and cell cycle and cytoskeleton functions (Figure 8B, MWCNT). In contrast, biological processes significantly regulated in response to TiO_2-NB showed differential regulation of inflammation involved neutrophil activation, and immune response involved phagocytosis, among other functions (Figure 8B, TiO_2-NB).

Of all the genes differentially regulated by both particle types at either the 1 h or 24 h time-point, 23 genes were significantly regulated in opposite directions ($p<0.05$) by MWCNT and TiO_2-NB compared to controls (Figure 9). These genes were primarily identified in THP-1 cells; however some were also differentially regulated in SAE and Caco-2/HT29-MTX cells. Network analysis using Dijkstra's shortest paths algorithm (Metacore) revealed that most genes (18 out of 23) are known to be associated with the transcription factors arylhydrocarbon receptor (AhR) and specificity protein 1 (Sp1) indicating that both NPs may function through a common mechanism with opposite outcomes.

Discussion

The main new findings to emerge from this work are the unique cell-specific response pattern of different cell types to the very same MWCNT and TiO_2-NB exposure, and the trend observed in all three cell-types, where the early (1h) response was common to both NP types, whereas the late (24 h) response was NP-specific, with most genes differentially

regulated in response to TiO_2-NB. This work also identified biological processes that were significantly regulated by both or either one of the NP types and might serve as general response mechanisms to NPs or NP-specific mechanisms underlying low or high levels of cytotoxicity.

Our study focused on three human cell types representing cells most likely to be impacted by NP exposure, including immune surveillance and epithelial cells lining the respiratory and intestinal tracts. The toxicity assessment studies in THP-1 cells confirmed the previously observed low and high level of toxicity by MWCNT and TiO_2-NB, respectively (Xia *et al.* 2013). Likewise, our studies in SAE cells confirmed previous observations (Xia *et al.* 2013), showing low toxicity induced by MWCNT and high toxicity induced by TiO_2-NB in cells representing the respiratory tract (Figure 2). A fundamentally different response pattern was observed in Caco-2/HT29-MTX cells, showing low toxicity by both MWCNT and TiO_2-NB. Although no *in vitro* studies of TiO_2-NB have been reported in intestinal cells, studies reporting the response of these cells to various types of carbon nanotubes support our observations with MWCNT, showing significant toxicity only in response to doses higher than 100 μg/ml (Jos *et al.* 2009; Kulamarva *et al.* 2008; Ponti *et al.* 2010;). The low toxicity of TiO_2-NB in Caco-2/HT29-MTX cells could be explained by the fact that these cells were exposed to the NPs after reaching a post-confluent, fully differentiated stage (14-21 days post plating). At this stage, they provide a physiologically relevant monolayer characterized by tight junctions, high trans-epithelial electrical resistance, and considerable mucus secretion that covers the monolayer (Mahler *et al.* 2009; Walter *et al.* 1996). It is likely that their mature physiological stage and the presence of protective mucus at the time of exposure may account for the low toxicity observed.

While the genes and proteins differentially expressed after NP exposure were almost entirely unique to each cell type, we observed some overlap in significantly regulated biological processes that emerged from both the proteomic and transcriptomic datasets across cell types (Figure 5). One interesting example includes the Metacore apoptotic nucleus biological process visualized as a network in Figure 5C, which was significantly enriched across cell types only after TiO_2-NB exposure. This signaling network, which is mediated by NF-κB, includes genes and proteins known to be involved in regulating apoptosis, cell cycle arrest and DNA repair associated with DNA replication stress and stress-induced genomic instability (Osborn *et al.* 2002). In response to cellular insult, this DNA-replication or S-phase checkpoint pathway is activated to allow damage to be repaired prior to replication for maintenance of genomic integrity. However, the downstream cellular consequences for activation of this pathway are multi-fold and may result in cell cycle arrest, DNA repair or cell death. TiO_2 NPs have previously been associated with p53-mediated genotoxicity and genetic instability as measured by increased apoptosis, accumulation of p53 and induced y-H2AX foci and 8-hydroxy-2'-deoxyguanosine, which are indicative of DNA double strand breaks and oxidative DNA damage, respectively (Kong *et al.* 2008; Meena *et al.* 2012; Trouiller *et al.* 2009). TiO_2 NPs were also found to be genotoxic in HEPG2 cells through upregulation of DNA damage responsive genes (p53, MDM2, GADD45 and p21) resulting in DNA strand breaks and increased intracellular reactive oxygen species (Petkovic *et al.* 2011). In our study, two pathways associated with

oxidative stress, Nitric oxide signaling and Role of NADPH oxidase and ROS, were also significantly regulated uniquely by TiO_2-NB (Figures 5). These data support the cytotoxicity observed in our study after TiO_2-NB exposure, particularly in SAE and THP-1 cells, which is likely to result from genotoxic and oxidative stress mechanisms. TiO_2-NB might induce genotoxicity by initiating oxidative stress and inflammatory cytokines (such as IFNγ or TNFα), which have previously been found to inhibit DNA repair capacity (Jaiswal *et al.* 2000). To investigate this possibility in more detail, we examined the transcriptional differences between TiO_2-NB and MWCNT exposure focusing on the differential response of these NPs in THP-1 cells at 24 hr (Figure 8).

THP-1 cells showed the most robust transcriptional response to NP exposure with unique responses to each NP type at 24 h. THP-1 cells also showed differential cytotoxic response to each particle type with TiO_2-NB resulting in ~40% cell death ($p<0.001$) and MWCNT resulting in ~10% toxicity ($p<0.05$). Overall, only approximately 10% of all significantly regulated genes in THP-1 cells at 24 h were found to be in common between TiO_2-NB and MWCNT. The common genes were associated with immune response and apoptosis from external signals (including NF-κB, MAPK or PI3K) and suggest that these processes can be involved in cellular response underlying both low and high NP toxicity. Exposure to MWCNT uniquely regulated cell cycle and DNA damage pathways, while exposure to TiO_2-NB resulted in the unique regulation of inflammatory response pathways (Figure 8). We investigated the genes in these pathways more closely and found that all the genes in the pathways unique to MWCNT were up-regulated, indicating that pathways for cell proliferation (mediated by MYC and CDK1), DNA repair (mediated by CHEK1, RAD51 and TOP2A) and anti-apoptosis (mediated by BIRC5, also called survivin) are important and unique to MWCNT exposure. In contrast, the genes associated with pathways unique to TiO_2-NB showed up-regulation of inflammation/cellular stress (mediated by NF-κB, TNF and IL-8) and down regulation of cell localization and chemotaxis. These genes and pathways likely describe the primary mechanisms for cell survival and cytotoxicity observed in THP-1 cells after exposure to MWCNT and TiO_2-NB, respectively. Cytotoxicity of alveolar macrophages to TiO_2-NB was found previously to be associated with phagolysosomal disruption and inflammasome activation (Hamilton *et al.* 2009) and is likely to also be relevant for the macrophage-like THP-1 cells. These observations indicate that both particle types likely elicit a stress response; however, MWCNT uniquely regulates cell proliferation, anti-apoptotic and repair mechanisms associated with cell survival, while TiO_2-NB activate an inflammatory response associated with cytotoxicity.

A small subset of genes were differentially regulated in opposite directions by the two particle types (Figure 9). These genes are of particular interest because they indicate a common regulatory mechanism across NP types, which results in opposite outcomes. Using network analysis we found that these genes were closely associated with the Sp1/Ahr-dependent stress response, which is known to be induced by xenobiotic chemicals such as polycyclic aromatic hydrocarbons (Stevens *et al.* 2009). In particular, genes that are transcriptional targets of Ahr, including CYP1A1, CYP1B1 and ARNT2, were down-regulated by MWCNT and up-regulated by TiO_2-NB depending on time point and cell type. Both CYP1A1 and CYP1B1 expression and enzymatic activity were previously found to be

repressed in human A549, HepG2 or MCF-7 cells after exposure to SWCNT (Hitoshi *et al.* 2012). The authors found that SWCNT inhibited both basal and dioxin-induced P450 levels likely by preventing binding of activated Ahr to enhancer regions for these genes. Our data indicates that these genes are also uniquely regulated by MWCNT and TiO_2-NB either directly or as a consequence of stress response signaling through these transcriptional regulators.

Conclusion

We investigated mechanisms of cytotoxicity for two high aspect ratio NPs, MWCNT and TiO_2-NB, presenting low and high cytotoxicity, respectively, using global proteomic and transcriptomic analyses. Using three cell types that represent the most common routes of human exposure to NPs, we observed cell type-specific regulation of genes and proteins when exposed to the same NPs using identical reagents and protocols. We also observed patterns of response that were NP-independent at early time points, suggesting a generic early response to insult. In contrast, NP-specific responses were observed at later time points, describing mechanisms associated with differential toxicity. Both NP types are likely to elicit a stress response; however, MWCNT uniquely up-regulated cell proliferation, anti-apoptotic and DNA repair mechanisms associated with cell survival, while TiO_2-NB differentially regulated inflammatory responses associated with cellular stress. In particular, our data shows that TiO_2-NB uniquely activated the NF-κB-mediated signaling pathway consisting of genes and proteins associated with apoptosis, cell cycle arrest and DNA repair related to DNA replication stress and genomic instability. The data also point to oxidative stress responses associated with inflammatory cytokines, such as IFNγ or TNFα, as possible mechanisms underlying TiO_2-NB toxicity. In support of these mechanistic distinctions, we also observed a subset of genes regulated in opposite directions between the two NP types. These genes were part of a stress response signaling network mediated by Sp1 and Ahr, known to be induced by xenobiotic chemicals. Overall, this unbiased approach allowed us to decipher differences in responses of three different cell-types to the exact same particle properties and identify mechanisms likely to underlie high vs. low toxicity of high aspect ratio NPs.

Supplementary Material

Refer to Web version on PubMed Central for supplementary material.

Acknowledgments

We thank Dr. Srikanth S. Nadadur at the National Institute of Environmental Health Sciences (NIEHS) who conceived the ideas for this study and provided critical guidance, insight and support. We thank Dr. Somenath Mitra at New Jersey Institute of Technology for providing the MWCNT, and Dr. Nianqiang Wu at West Virginia University for providing the TiO_2-NB, as part of the NIEHS Nanotechnology Environmental Health and Safety consortium effort. Part of this research was performed using EMSL, a national scientific user facility sponsored by the Department of Energy's Office of Biological and Environmental Research and located at Pacific Northwest National Laboratory.

Funding

This work was supported by the National Institute of Environmental Health Sciences [RC2ES018025-01S1 to F.A.W.], [RC2ES018742-01S1 to A.H.] and [1RC2ES018786-01S1 to G.O.]

References

Benjamini Y, Hochberg Y. Controlling the false discovery rate - a practical and powerful approach to multiple testing. J Roy Stat Soc B Met. 1995; 57:289–300.

Blazer-Yost BL, Banga A, Amos A, Chernoff E, Lai XY, Li C, Mitra S, Witzmann FA. Effect of carbon nanoparticles on renal epithelial cell structure, barrier function, and protein expression. Nanotoxicology. 2011; 5:354–371. [PubMed: 21067278]

Bolstad BM, Irizarry RA, Astrand M, Speed TP. A comparison of normalization methods for high density oligonucleotide array data based on variance and bias. Bioinformatics. 2003; 19:185–193. [PubMed: 12538238]

Chen Y, Mitra S. Fast microwave-assisted purification, functionalization and dispersion of multi-walled carbon nanotubes. J Nanosci Nanotechnol. 2008; 8:5770–5775. [PubMed: 19198303]

Donaldson K, Borm PJA, Oberdorster G, Pinkerton KE, Stone V, Tran CL. Concordance between in vitro and in vivo dosimetry in the proinflammatory effects of low toxicity, low-solubility particles: The key role of the proximal alveolar region. Inhal Toxicol. 2008; 20:53–62. [PubMed: 18236223]

Donaldson K, Murphy F, Schinwald A, Duffin R, Poland CA. Identifying the pulmonary hazard of high aspect ratio nanoparticles to enable their safety-by-design. Nanomedicine-Uk. 2011; 6:143–156.

Hamilton RF, Girtsman TA, Xiang C, Wu N, Holian A. Nickel Contamination on MWCNT is Related to Particle Bioactivity but not Toxicity in the THP-1 transformed Macrophage Model. Int J Biomed Nanosci Nanotech. 2012 (in press).

Hamilton RF, Wu N, Porter D, Buford M, Wolfarth M, Holian A. Particle length-dependent titanium dioxide nanomaterials toxicity and bioactivity. Part Fibre Toxicol. 2009; 6:35. [PubMed: 20043844]

Helland A, Wick P, Koehler A, Schmid K, Som C. Reviewing the environmental and human health knowledge base of carbon nanotubes. Environ Health Persp. 2007; 115:1125–1131.

Hitoshi K, Katoh M, Suzuki T, Ando Y, Nadai M. Changes in expression of drug- metabolizing enzymes by single-walled carbon nanotubes in human respiratory tract cells. Drug Metab Dispos. 2012; 40:579–587. [PubMed: 22187486]

Iavicoli I, Leso V, Fontana L, Bergamaschi A. Toxicological effects of titanium dioxide nanoparticles: A review of in vitro mammalian studies. Eur Rev Med Pharmaco. 2011; 15:481–508.

Jaiswal M, LaRusso NF, Burgart LJ, Gores GJ. Inflammatory cytokines induce DNA damage and inhibit DNA repair in cholangiocarcinoma cells by a nitric oxide-dependent mechanism. Cancer Res. 2000; 60:184–190. [PubMed: 10646872]

Jia G, Wang HF, Yan L, Wang X, Pei RJ, Yan T, Zhao YL, Guo XB. Cytotoxicity of carbon nanomaterials: Single-wall nanotube, multi-wall nanotube, and fullerene. Environ Sci Technol. 2005; 39:1378–1383. [PubMed: 15787380]

Jos A, Pichardo S, Puerto M, Sanchez E, Grilo A, Camean AM. Cytotoxicity of carboxylic acid functionalized single wall carbon nanotubes on the human intestinal cell line caco-2 Toxicol in Vitro. 2009; 23:1491–1496.

Karakoti AS, Munusamy P, Hostetler K, Kodali V, Kuchibhatla S, Orr G, Pounds JG, Teeguarden JG, Thrall BD, Baer DR. Preparation and characterization challenges to understanding environmental and biological impacts of nanoparticles. Surf Interface Anal. 2012; 44:882–889. [PubMed: 23430137]

Keller A, Nesvizhskii AI, Kolker E, Aebersold R. Empirical statistical model to estimate the accuracy of peptide identifications made by ms/ms and database search. Anal Chem. 2002; 74:5383–5392. [PubMed: 12403597]

Kong SJ, Kim BM, Lee YJ, Chung HW. Titanium dioxide nanoparticles trigger p53- mediated damage response in peripheral blood lymphocytes. Environ Mol Mutagen. 2008; 49:399–405. [PubMed: 18418868]

Kulamarva A, Bhathena J, Malhotra M, Sebak S, Nalamasu O, Ajayan P, Prakash S. In vitro cytotoxicity of functionalized single walled carbon nanotubes for targeted gene delivery applications. Nanotoxicology. 2008; 2:184–188.

Lai XY, Wang LS, Tang HX, Witzmann FA. A novel alignment method and multiple filters for exclusion of unqualified peptides to enhance label-free quantification using peptide intensity in lc-ms/ms. J Proteome Res. 2011; 10:4799–4812. [PubMed: 21888428]

Magrez A, Horvath L, Smajda R, Salicio V, Pasquier N, Forro L, Schwaller B. Cellular toxicity of tio_2-based nanofilaments. Acs Nano. 2009; 3:2274–2280. [PubMed: 19610603]

Mahler GJ, Shuler ML, Glahn RP. Characterization of CaCO-2 and HT29-MTX cocultures in an in vitro digestion/cell culture model used to predict iron bioavailability. J Nutr Biochem. 2009; 20:494–502. [PubMed: 18715773]

Meena R, Rani M, Pal R, Rajamani P. Nano-tio2-induced apoptosis by oxidative stress-mediated DNA damage and activation of p53 in human embryonic kidney cells. Appl Biochem Biotech. 2012; 167:791–808.

Mercer R R, Hubbs AF, Scabilloni JF, Wang LY, Battelli LA, Schwegler-Berry D, Castranova V, Porter DW. Distribution and persistence of pleural penetrations by multi-walled carbon nanotubes. Part Fibre Toxicol. 2010; 7:28. [PubMed: 20920331]

Murr LE, Garza KM, Soto KF, Carrasco A, Powell TG, Ramirez DA, Guerrero PA, Lopez DA, Venzor J 3rd. Cytotoxicity assessment of some carbon nanotubes and related carbon nanoparticle aggregates and the implications for anthropogenic carbon nanotube aggregates in the environment. Int J Environ Res Public Health. 2005; 2:31–42. [PubMed: 16705799]

Nesvizhskii AI, Keller A, Kolker E, Aebersold R. A statistical model for identifying proteins by tandem mass spectrometry. Anal Chem. 2003; 75:4646–4658. [PubMed: 14632076]

Oberdörster G, Donaldson K, Castranova V, Fitzpatrick J, Ausman K, Carter J, Karn B, Kreyling W, Lai D, Olin S, Monteiro-Riviere N, Warheit D, Yang H. Principles for characterizing the potential human health effects from exposure to nanomaterials: Elements of a screening strategy. Part Fibre Toxicol. 2005; 2:8. [PubMed: 16209704]

Osborn AJ, Elledge SJ, Zou L. Checking on the fork: The DNA-replication stress-response pathway. Trends Cell Biol. 2002; 12:509–516. [PubMed: 12446112]

Pacurari M, Castranova V, Vallyathan V. Single-and multi-wall carbon nanotubes versus asbestos: Are the carbon nanotubes a new health risk to humans? J Toxicol Env Heal A. 2010; 73:378–395.

Petković J, Zegura B, Stevanović M, Drnovšek N, Uskoković D, Novak S, Filipič M. DNA damage and alterations in expression of DNA damage responsive genes induced by TiO_2 nanoparticles in human hepatoma HepG2 cells. Nanotoxicology. 2011; 5(3):341–53. [PubMed: 21067279]

Ponti J, Colognato R, Rauscher H, Gioria S, Broggi F, Franchini F, Pascual C, Giudetti G, Rossi F. Colony forming efficiency and microscopy analysis of multi-wall carbon nanotubes cell interaction. Toxicol Lett. 2010; 197:29–37. [PubMed: 20435104]

Pulskamp K, Diabate S, Krug HF. Carbon nanotubes show no sign of acute toxicity but induce intracellular reactive oxygen species in dependence on contaminants. Toxicol Lett. 2007; 168:58–74. [PubMed: 17141434]

Saeed AI, Sharov V, White J, Li J, Liang W, Bhagabati N, Braisted J, Klapa M, Currier T, Thiagarajan M, Sturn A, Snuffin M, Rezantsev A, Popov D, Ryltsov A, Kostukovich E, Borisovsky I, Liu Z, Vinsavich A, Trush V, Quackenbush J. Tm4: A free, open-source system for microarray data management and analysis. Biotechniques. 2003; 34:374–378. [PubMed: 12613259]

Shvedova AA, Kisin ER, Porter D, Schulte P, Kagan VE, Fadeel B, Castranova V. Mechanisms of pulmonary toxicity and medical applications of carbon nanotubes: Two faces of janus? Pharmacol Therapeut. 2009; 121:192–204.

Soto K, Garza KM, Murr LE. Cytotoxic effects of aggregated nanomaterials. Acta Biomater. 2007; 3:351–358. [PubMed: 17275430]

Stevens EA, Mezrich JD, Bradfield CA. The aryl hydrocarbon receptor: A perspective on potential roles in the immune system. Immunology. 2009; 127:299–311. [PubMed: 19538249]

Storey JD. A direct approach to false discovery rates. J Roy Stat Soc B. 2002; 64:479–498.

Thurnherr T, Brandenberger C, Fischer K, Diener L, Manser P, Maeder-Althaus X, Kaiser JP, Krug HF, Rothen-Rutishauser B, Wick P. A comparison of acute and long-term effects of industrial multiwalled carbon nanotubes on human lung and immune cells in vitro. Toxicol Lett. 2011; 200:176–186. [PubMed: 21112381]

Tilton SC, Tal TL, Scroggins SM, Franzosa JA, Peterson ES, Tanguay RL, Waters KM. Bioinformatics Resource Manager v2.3: An integrated software environment for systems biology with microRNA and cross-species analysis tools. BMC Bioinformatics. 2012; 13:311. [PubMed: 23174015]

Trouiller B, Reliene R, Westbrook A, Solaimani P, Schiestl RH. Titanium dioxide nanoparticles induce DNA damage and genetic instability in vivo in mice. Cancer Res. 2009; 69:8784–8789. [PubMed: 19887611]

Verma D, Sarndahl E, Andersson H, Ericksson P, Fredrikson M, Jonsson JI, Lerm M, Soderkvist P. The Q705K polymorphism in NLRP3 is a gain-of-function alteration leading to excessive interleukin-1β and IL-18 production. PLoS One. 2012; 7(4)

Walter E, Janich S, Roessler BJ, Hilfinger JM, Amidon GL. HT29-MTX/CaCO-2 cocultures as an in vitro model for the intestinal epithelium: In vitro in vivo correlation with permeability data from rats and humans. J Pharm Sci. 1996; 85:1070–1076. [PubMed: 8897273]

Wang J, Tafen DN, Lewis JP, Hong ZL, Manivannan A, Zhi MJ, Li M, Wu NQ. Origin of photocatalytic activity of nitrogen-doped TiO_2 nanobelts. J Am Chem Soc. 2009; 131:12290–12297. [PubMed: 19705915]

Wang X, Xia TA, Ntim SA, Ji ZX, George S, Meng HA, Zhang HY, Castranova V, Mitra S, Nel AE. Quantitative techniques for assessing and controlling the dispersion and biological effects of multiwalled carbon nanotubes in mammalian tissue culture cells. Acs Nano. 2010; 4:7241–7252. [PubMed: 21067152]

Warheit DB, Webb TR, Sayes CM, Colvin VL, Reed KL. Pulmonary instillation studies with nanoscale TiO_2 rods and dots in rats: Toxicity is not dependent upon particle size and surface area. Toxicol Sci. 2006; 91:227–236. [PubMed: 16495353]

Watanabe M, Okada M, Kudo Y, Tonori Y, Niitsuya M, Sato T, Aizawa Y, Kotani M. Differences in the effects of fibrous and particulate titanium dioxide on alveolar macrophages of fischer 344 rats. J Toxicol Env Heal A. 2002; 65:1047–1060.

Wikmanlarhed A, Artursson P. Cocultures of human intestinal goblet (HT29-H) and absorptive (CaCO-2) cells for studies of drug and peptide absorption. Eur J Pharm Sci. 1995; 3:171–183.

Xia, T.; Hamilton, JR.; Bonner, J.; Crandall, E.; Elder, A.; Fazlollahi, F.; Girtsman, T.; Kim, K.; Mitra, S.; Ntim, S.; Orr, G.; Tagmount, M.; Taylor, A.; Telesca, D.; Tolic, A.; Vulpe, C.; Walker, A.; Wang, X.; Witzmann, F.; Wu, N.; Xie, Y.; Nel, A.; Holian, A. Inter-laboratory comparison of in vitro nanotoxicological assays from the NIEHS NanoGO consortium. Environ Health Persp. Online Advance Publicaiton; Apr. 2013 2013 in press

Xie Y, Williams NG, Tolic A, Chrisler WB, Teeguarden JG, Maddux BL, Pounds JG, Laskin A, Orr G. Aerosolized ZnO nanoparticles induce toxicity in alveolar type II epithelial cells at the air-liquid interface. Toxicol Sci. 2012; 125:450–61. [PubMed: 21964423]

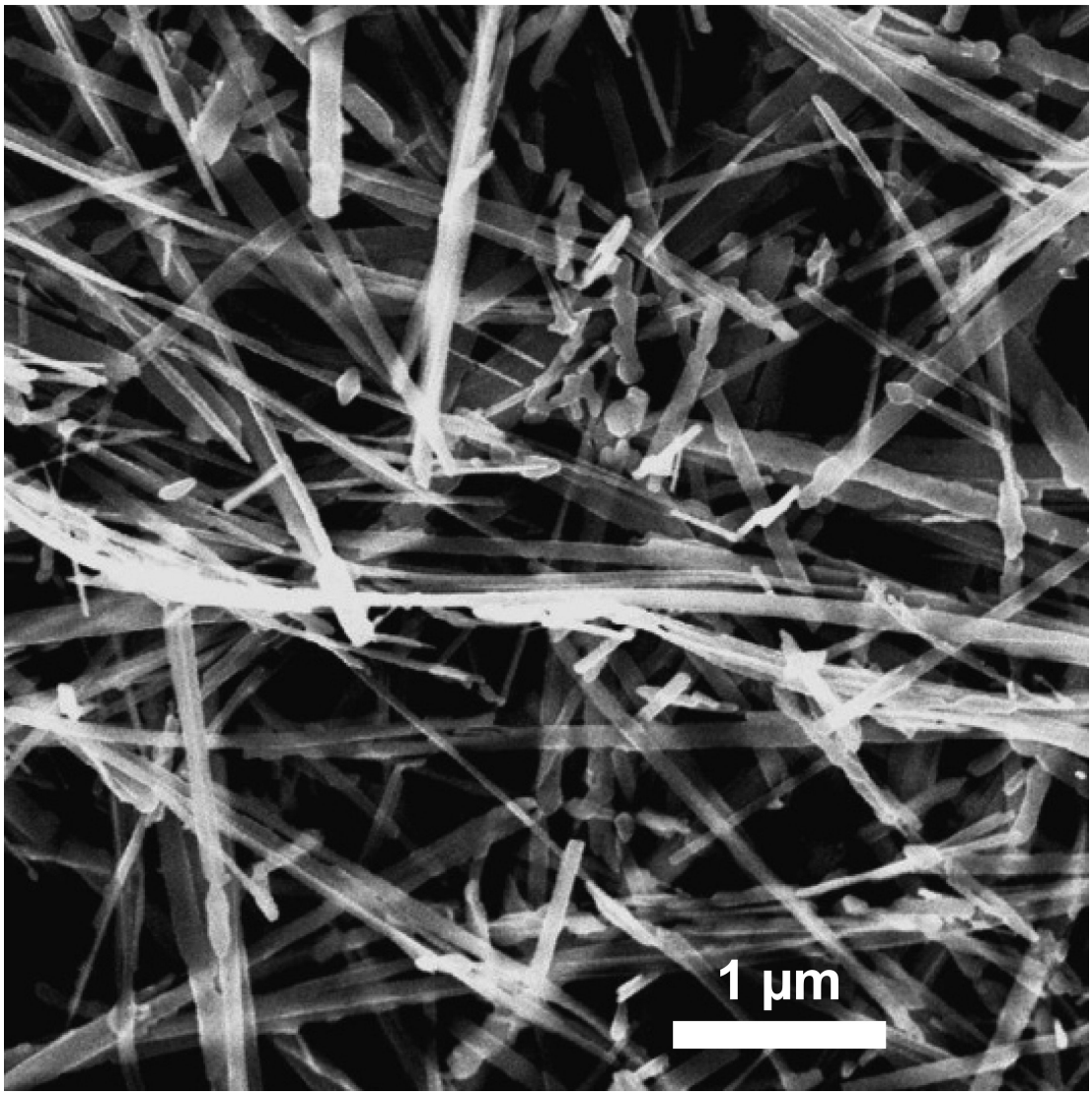

Figure 1.
Transmission electron microscopy image of the TiO_2-NB used in this study.

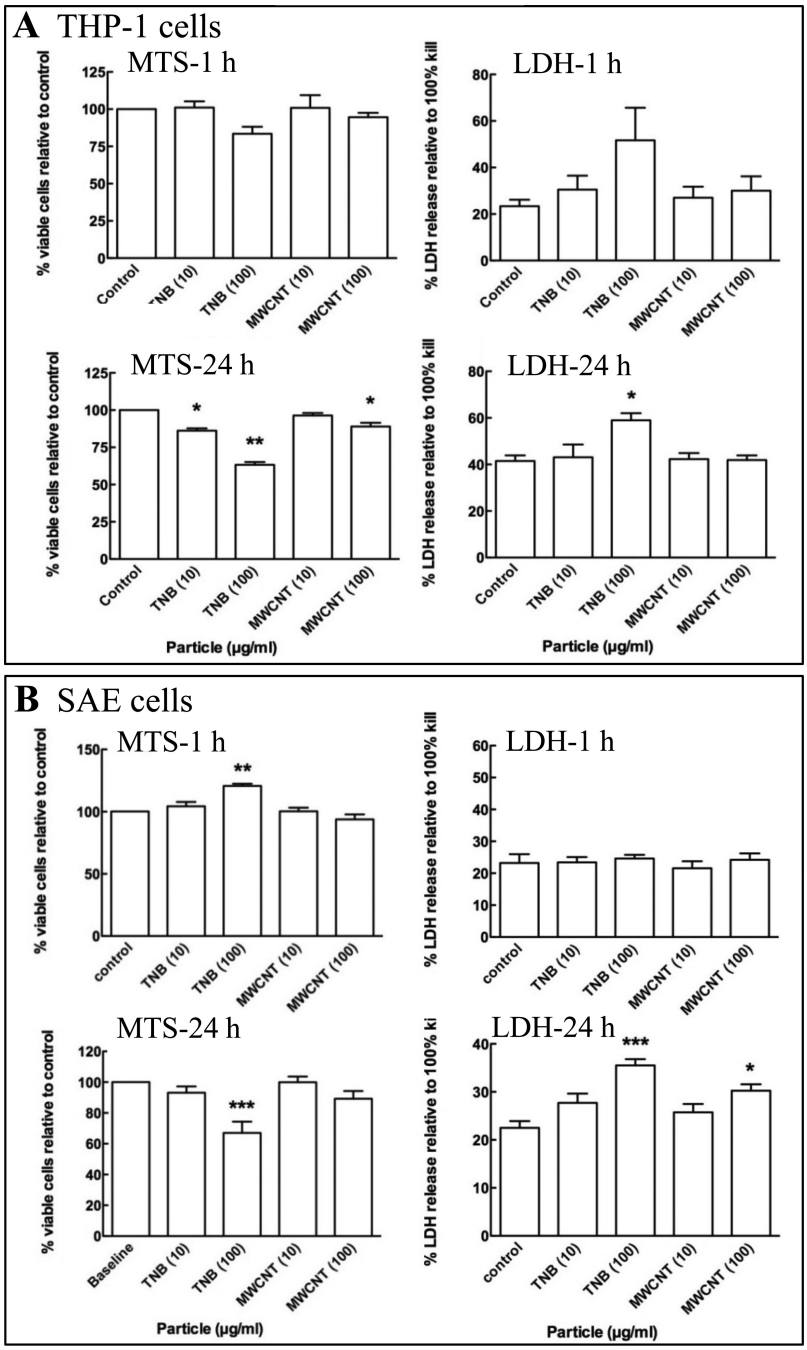

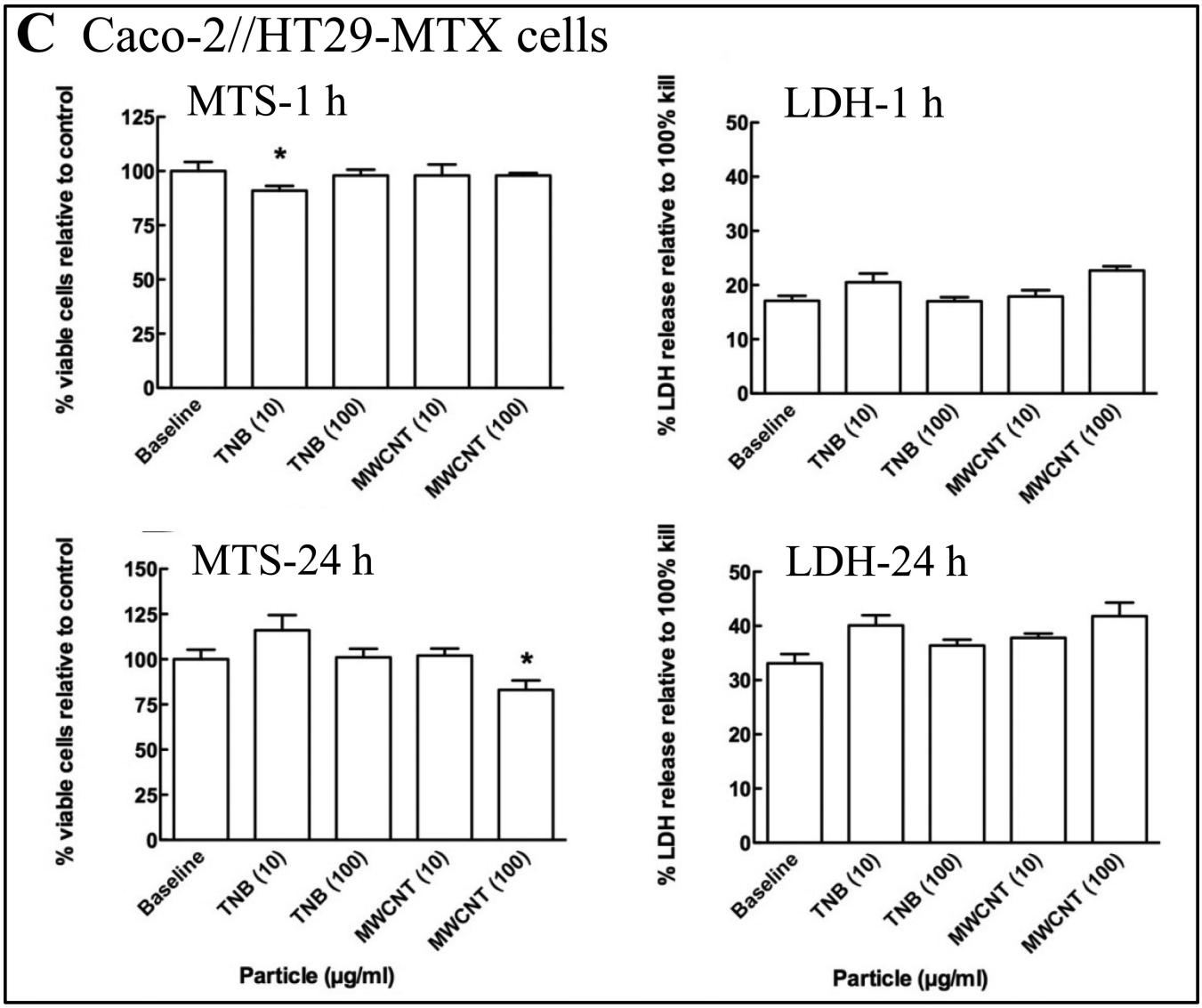

Figure 2.

The percent viable THP-1 (A), SAE (B) and Caco-2/HT29-MTX (C) cells relative to control was quantified by measuring the reduction of MTS to formazan in metabolically active cells at 1 h (MTS-1 h) and 24 h (MTS-24 h) post exposure to MWCNT and TiO_2-NB (TNB). Membrane integrity relative to control was quantified by the LDH release assay at 1 h (LDH-1 h) and 24 h (LDH-24 h) post exposure to MWCNT and TiO_2-NB (TNB). Significance, indicated at $P < 0.05$ (*), $P < 0.01$ (**) or $P < 0.001$ (***), was determined using a one-way ANOVA and presented as the standard error of the mean (SEM).

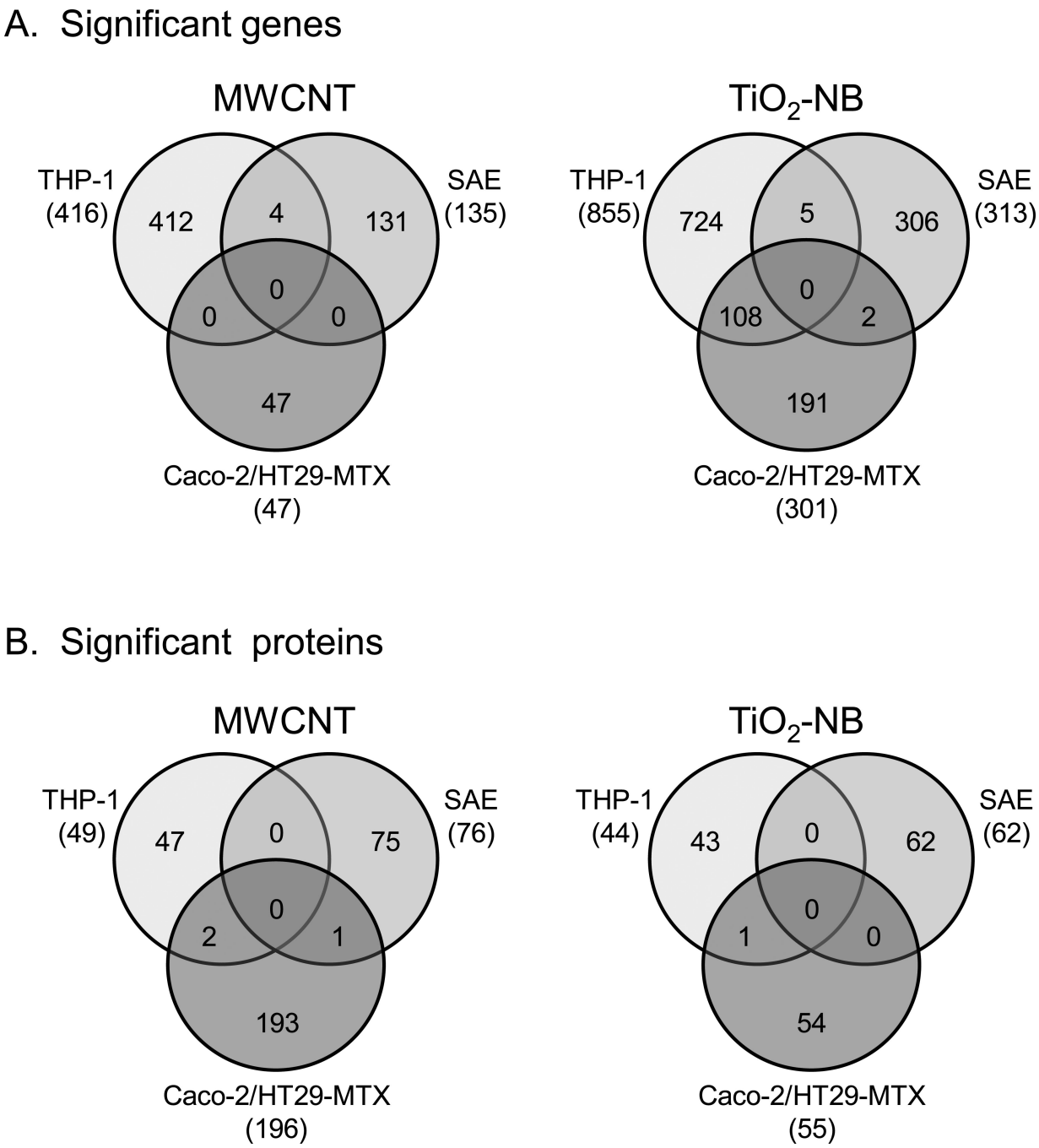

Figure 3.

Significantly regulated genes and proteins are unique to each cell type after exposure to MWCNT or TiO_2-NB. Venn diagrams of all genes (A) and proteins (B) differentially expressed ($p<0.05$, 1.5-fold change compared to controls), showing no overlap across all three cell-types.

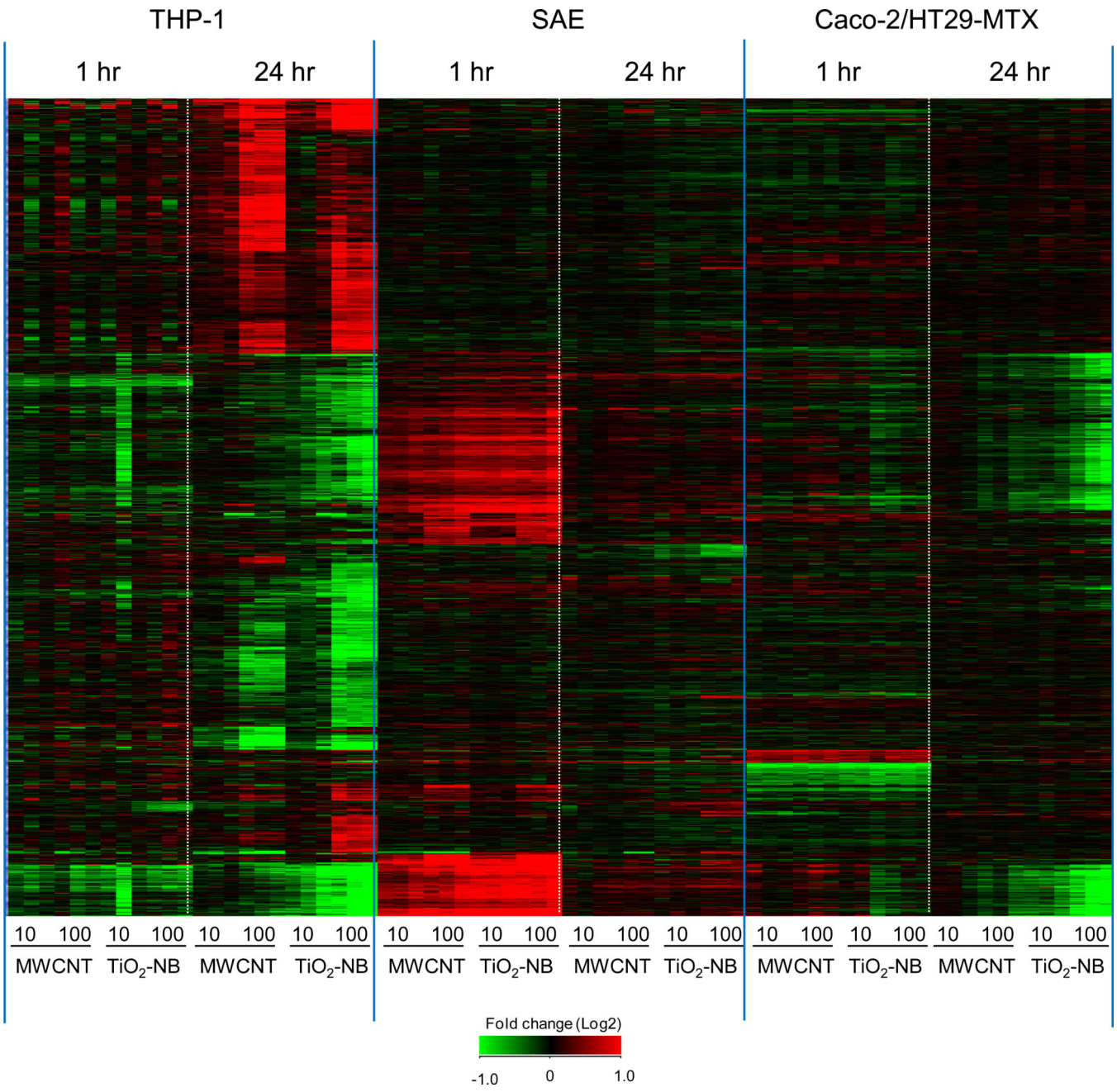

Figure 4.

Hierarchical clustering of 1479 differentially expressed ($p<0.05$, 1.5-fold change) genes after exposure to 10 or 100 μg/ml MWCNT or TiO_2-NB for 1 h or 24 h. Values are fold change (Log2) compared to cell- and time-matched controls. Red indicates up-regulated genes, green indicates down-regulated genes, and black indicates no change.

A

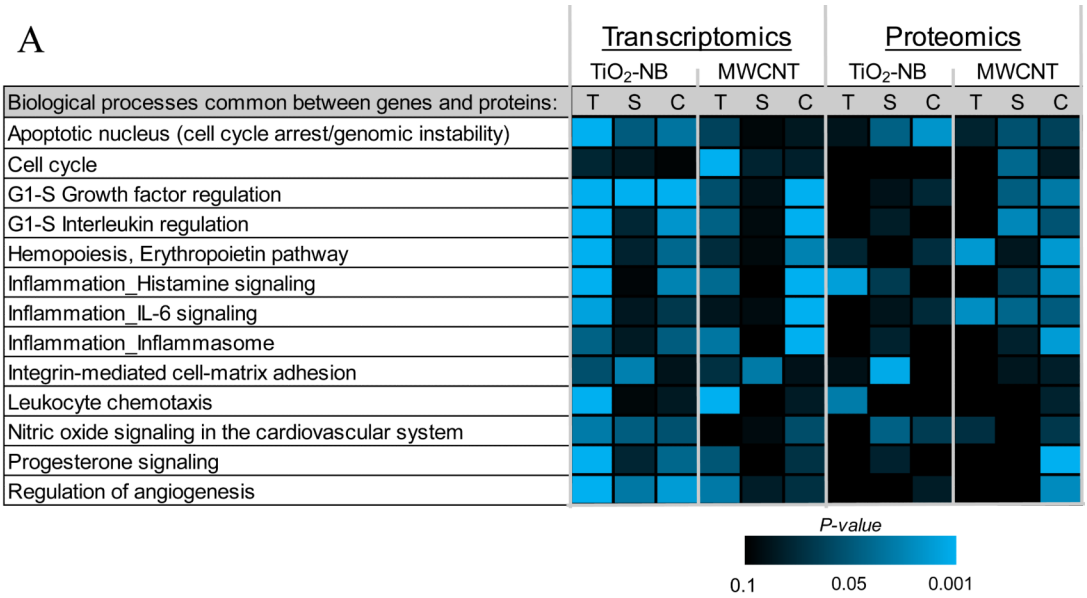

B

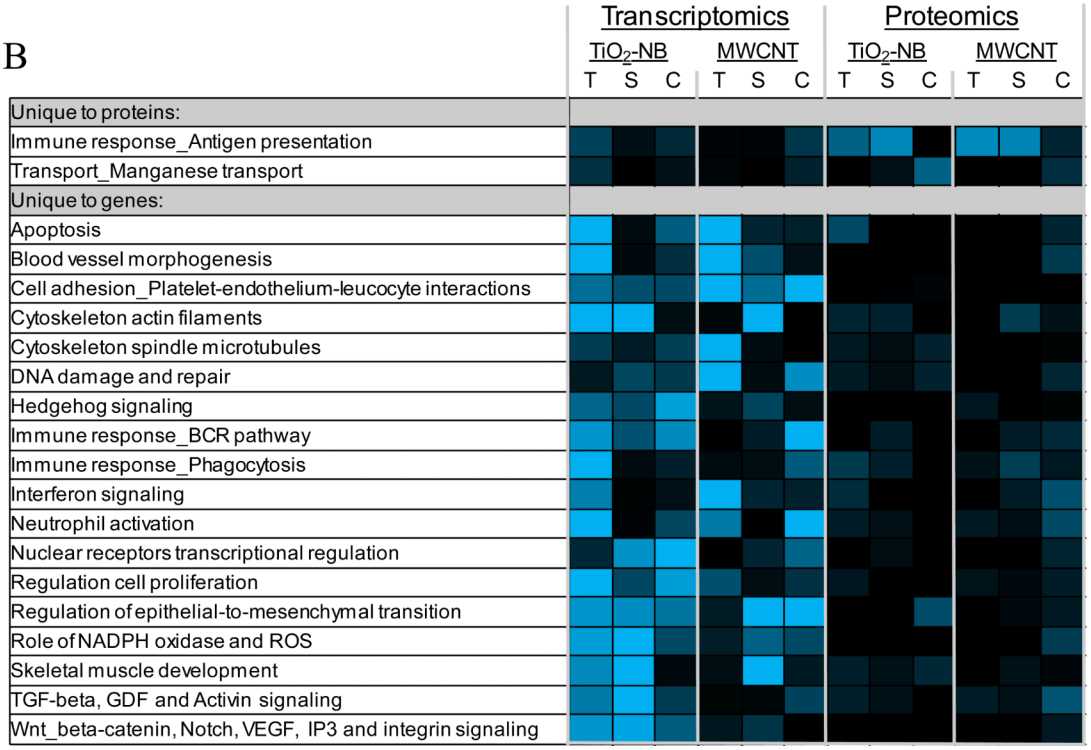

C

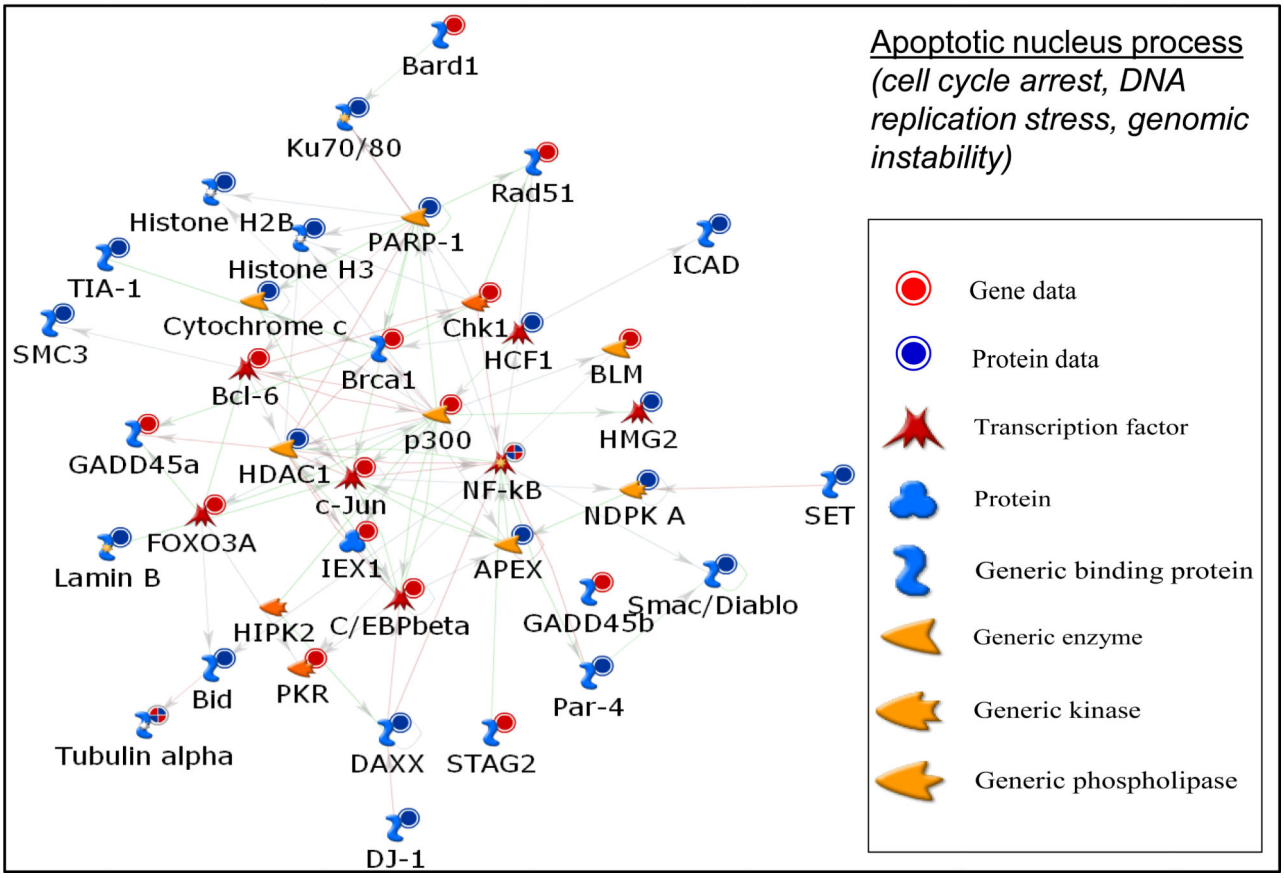

Figure 5.

A. All significantly enriched biological processes at both the transcriptional and proteomic level across cell types (T, THP-1; S, SAE; C, Caco-2/MTX) after exposure to TiO_2-NB or MWCNT. Functional enrichment of significantly regulated genes and proteins was performed in MetaCore (GeneGO). The heatmap represents the *P*-value significance level of each biological process across all conditions; black is non-significant and blue is highly significant ($p<0.001$). **B.** Significant enriched biological processes unique for transcriptional or proteomic datasets across cell types (T, THP-1; S, SAE; C, Caco-2/MTX) after exposure to TiO_2-NB or MWCNT. Functional enrichment of significantly regulated genes and proteins was performed in MetaCore (GeneGO). The heatmap represents the *P*-value significance level of each biological process. **C.** A Metacore network visualization of the differentially regulated genes (red circles) and proteins (blue circles) in the Apoptotic_nucleus biological process created using the direct interactions among the nodes.

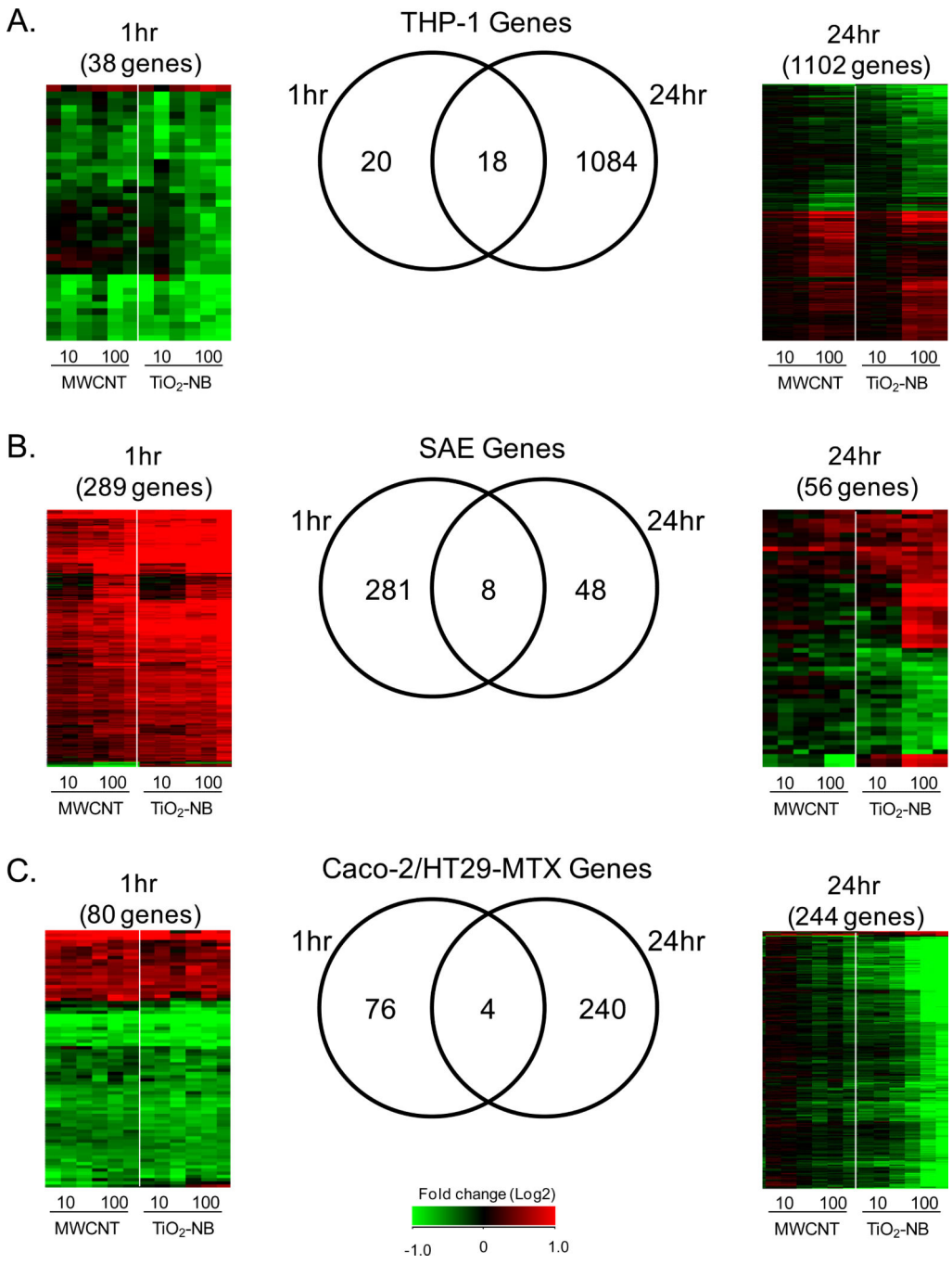

Figure 6.

In all three cell types, the early transcriptional response (1 hr) is primarily common across nanoparticle type while the late response (24 hr) is unique, mostly in respone to TiO_2-NB. Venn diagrams and heatmaps of significantly regulated genes ($p<0.05$, 1.5-fold change) are shown at each time-point for THP-1 (A), SAE cells (B) and Caco-2/HT29-MTX (C). Values in heatmaps are fold-change (Log2) compared to time- and cell-matched controls. Red indicates up-regulated genes, green indicates down-regulated genes, and black indicates no change.

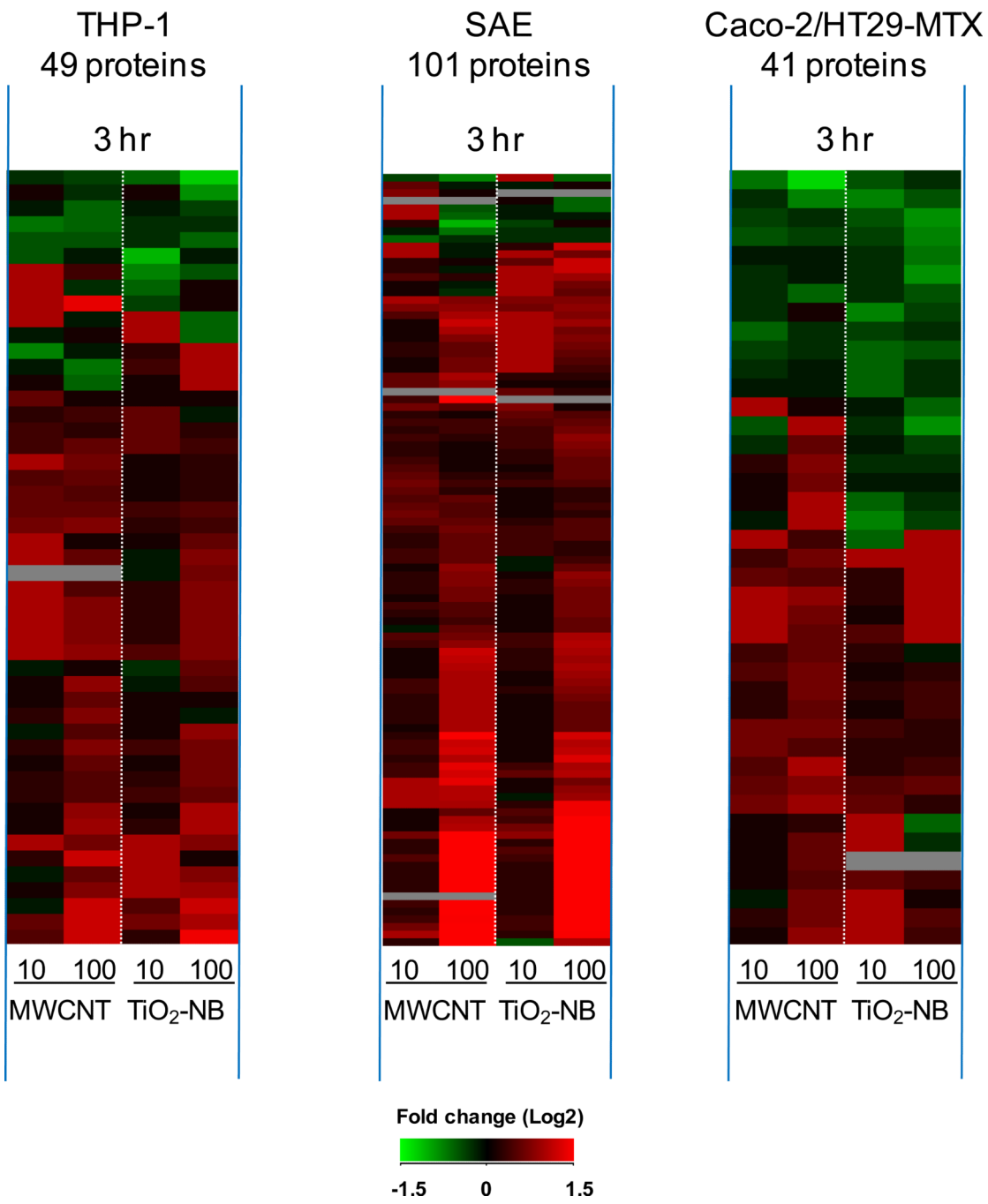

Figure 7.

In all three cell types, the early proteomic response (3 hr) is primarily common across nanoparticle type. Heatmaps show significantly regulated proteins ($p<0.05$, 1.5-fold change) for THP-1, SAE cells and Caco-2/HT29-MTX after 3 h exposure to MWCNT or TiO_2-NB. Values are fold-change (Log2) compared to time- and cell-matched controls. Red indicates increased protein abundance, green indicates decreased protein abundance, and black indicates no change.

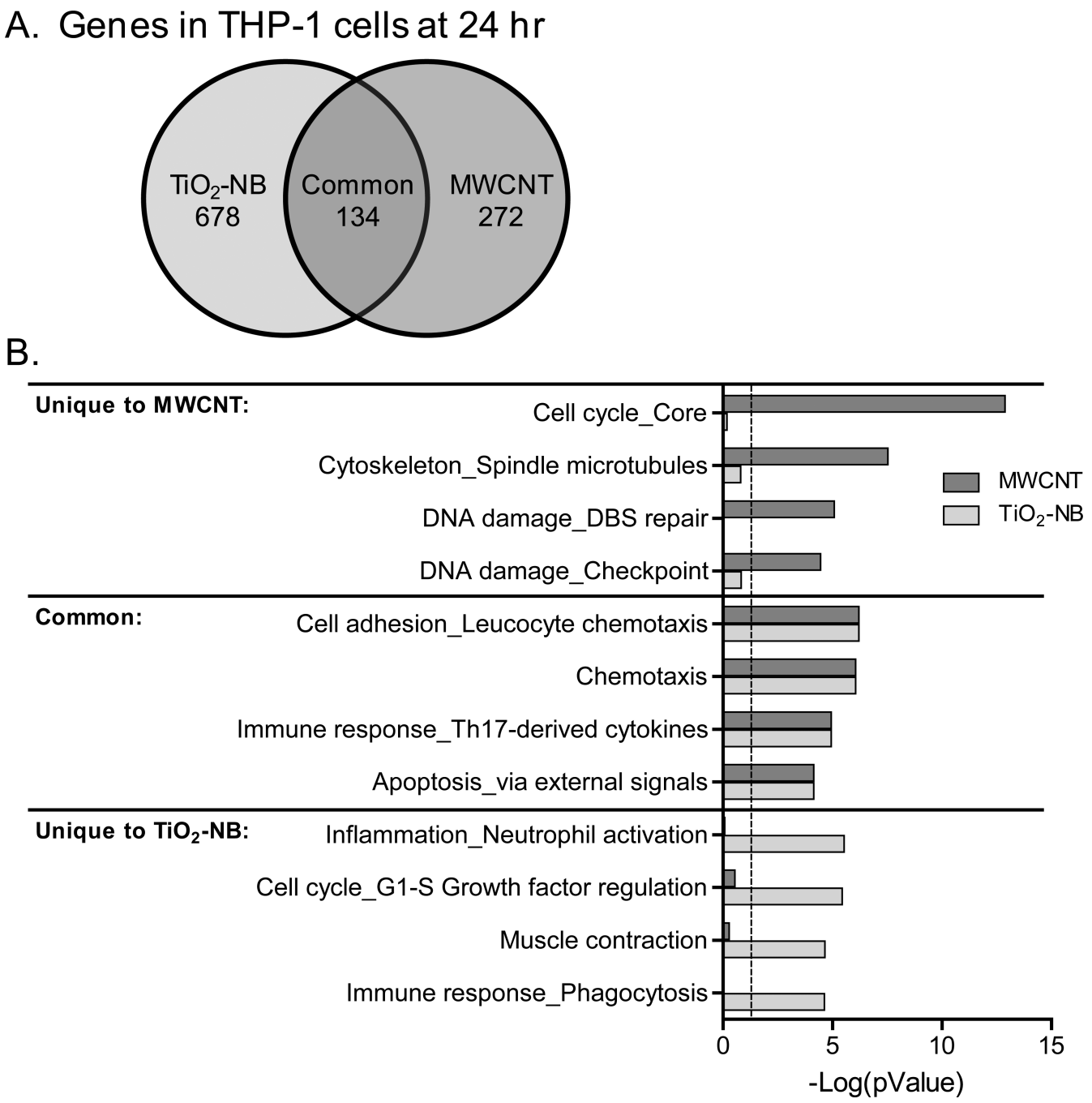

Figure 8.

TiO_2-NB and MWCNT elicit unique signatures in THP-1 cells at 24 hr, describing mechanisms that might underlie NP toxicity or biocompatibility. **A.** Venn diagram of significantly regulated genes ($p<0.05$, 1.5-fold change) in THP-1 cells at 24 h in response to TiO_2-NB and MWCNT. **B.** Significantly regulated biological processes ($p<0.05$) in response to TiO_2-NB (blue bars) and MWCNT (orange bars). Functional enrichment of significantly regulated genes was performed in MetaCore (GeneGO) and the top four biological processes

based on significance level are shown for processes unique to each NP or common to both NP type. Values are –log(pValue) and dashed line indicates significance level of $p<0.05$.

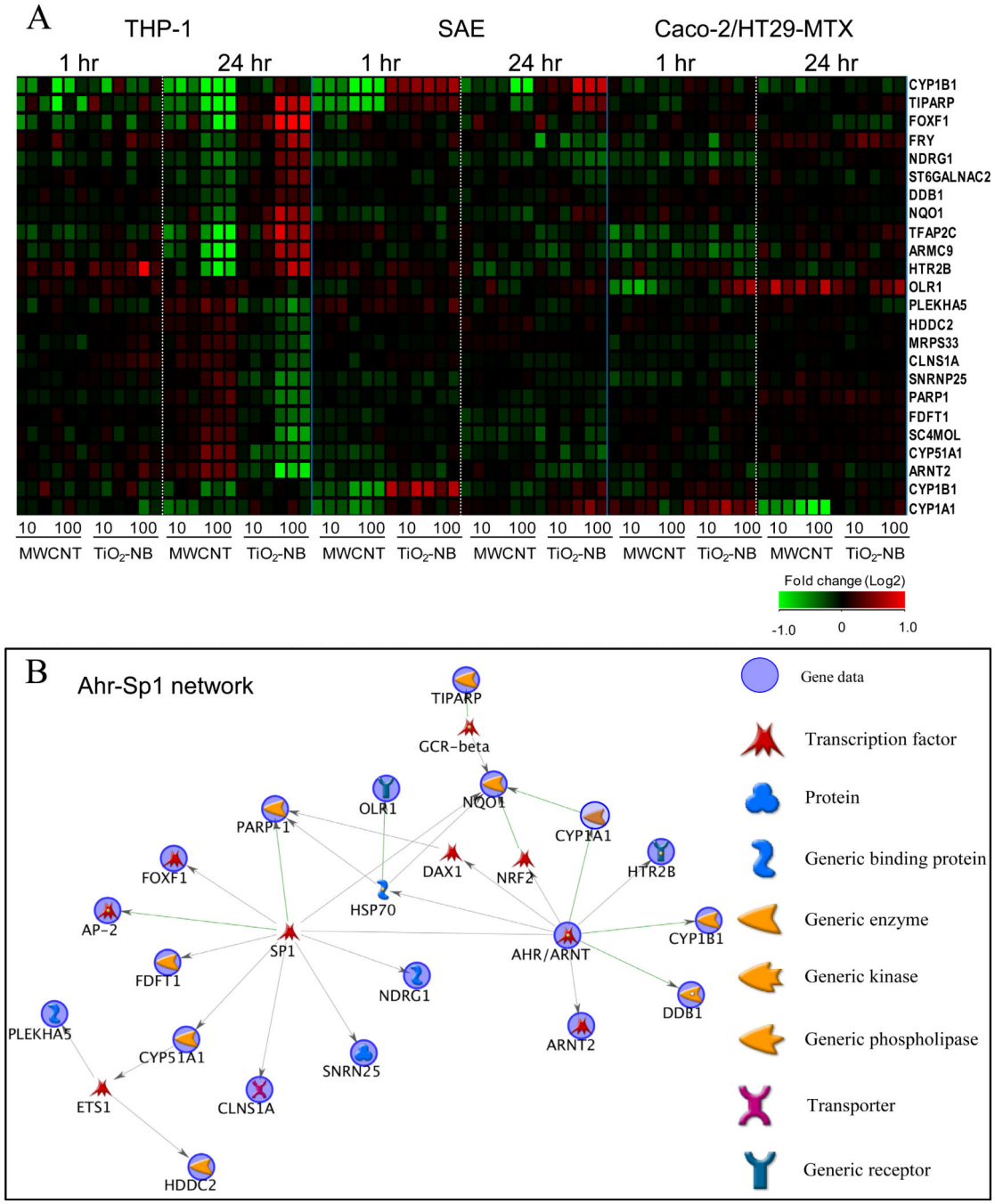

Figure 9.

All genes significantly regulated ($p<0.05$) in opposite directions by MWCNT and TiO_2-NB exposure. **A.** Heatmap of differential gene regulation. Values are fold change (Log2) compared to cell- and time-matched controls. Red indicates up-regulated genes, green indicates down-regulated genes, and black indicates no change. **B.** Visualization of these genes in a biological network showing that most genes are associated with the stress

response mediated by AhR and Sp1 transcription factors. Genes from the experimental data significantly regulated by NP exposure are highlighted with a blue circle.

Table I

Experimental Design

Cells	NPs	μg/ml	Exposure[a]
Hu macrophage like THP-1	MWCNT, TiO_2 nanobelt	10, 100	1 or 3, 24 hr
Hu small airway epithelial cells	MWCNT, TiO_2 nanobelt	10, 100	1 or 3, 24 hr
Hu Caco-2/HT29-MTX	MWCNT, TiO_2 nanobelt	10, 100	1 or 3, 24 hr

[a]Samples for transcriptomics were collected after 1 and 24 hr exposures. Samples for proteomics were collected after 3 and 24 hr exposures.

Table II

NP Characterization

Measurement	MWCNT	TiO_2-NB
Size in H_2O (nm)	858±58	2897±117
Size in RPMI (nm)	375±23	1590±126
Size in SEGM (nm)	342±86	445±42.5
Size in DMEM (nm)	458±16	634±86
Zeta potential in H_2O (mV)	−11.8±1.1	−30.3±2.8
Zeta potential in RPMI (mV)	−9.78±1.1	−12.7±4.7
Zeta potential in SEGM (mV)	−13.3±0.6	−11.6±1.0
Zeta potential in DMEM (mV)	−10.64±1.0	−9.45±0.4

Size (mean nm ± range) was measured by Dynamic Light Scattering and zeta potential (mean mV ± s.d.) was measured by Zetasizer.